



HAL
open science

Steady shear viscosity of blends of fresh and RAP binders with rejuvenator: Experimental and estimated results

A. Forton, S. Mangiafico, C. Sauzéat, H. Di Benedetto, P. Marc

► To cite this version:

A. Forton, S. Mangiafico, C. Sauzéat, H. Di Benedetto, P. Marc. Steady shear viscosity of blends of fresh and RAP binders with rejuvenator: Experimental and estimated results. *Construction and Building Materials*, 2021, 269, pp.121236 -. 10.1016/j.conbuildmat.2020.121236 . hal-03493832

HAL Id: hal-03493832

<https://hal.science/hal-03493832>

Submitted on 2 Jan 2023

HAL is a multi-disciplinary open access archive for the deposit and dissemination of scientific research documents, whether they are published or not. The documents may come from teaching and research institutions in France or abroad, or from public or private research centers.

L'archive ouverte pluridisciplinaire **HAL**, est destinée au dépôt et à la diffusion de documents scientifiques de niveau recherche, publiés ou non, émanant des établissements d'enseignement et de recherche français ou étrangers, des laboratoires publics ou privés.



Distributed under a Creative Commons Attribution - NonCommercial 4.0 International License

1 Steady shear viscosity of blends of fresh and RAP binders with rejuvenator: 2 experimental and estimated results

3 A. Forton^{a,b*}, S. Mangiafico^a, C. Sauzéat^a, H. Di Benedetto^a, P. Marc^b

4 ^a Université de Lyon/ENTPE, LTDS (UMR CNRS 5513), rue Maurice Audin, 69518 Vaulx-en-
5 Velin Cedex, France;

6 ^b University Politehnica Timisoara, Piata Victoriei, 300006 Timisoara, Romania;
7 andrei.forton@student.upt.ro; salvatore.mangiafico@entpe.fr; cedric.sauzeat@entpe.fr;
8 herve.dibenedetto@entpe.fr; paul.marc@upt.ro

9 * corresponding author

10

11 Abstract

12 This paper focuses on the influence of the RAP-extracted binder and rejuvenator contents on the
13 steady shear viscosity obtained as a linear viscoelastic property of different binder blends. One pure
14 fresh 50/70 binder, a RAP-extracted binder and a rejuvenator of vegetal origin were mixed in
15 different dosages. Steady shear viscosity (η_0) values at different temperatures (from 25°C to 85°C)
16 were determined from complex shear modulus results for all tested binders. In addition, $\eta_0(T)$
17 values of all binder blends were estimated from $\eta_0(T)$ values of base constituents by using two
18 different approaches. Good correspondences with experimental results were found.

19

20 **Keywords:** RAP binder; rejuvenator; steady shear viscosity; binder blends; estimations.

21

22 Highlights

- 23 • Viscoelastic properties (steady shear viscosity) of several binders were studied.
- 24 • Steady shear viscosity η_0 at 85°C was determined from complex shear modulus results.
- 25 • $\eta_0(T)$ were calculated from $\eta_0(T_{ref} = 85^\circ\text{C})$ and a_T shift factor at temperature T .
- 26 • $\eta_0(T)$ of all binder blends were estimated with two different approaches.

27

28

29 1. Introduction

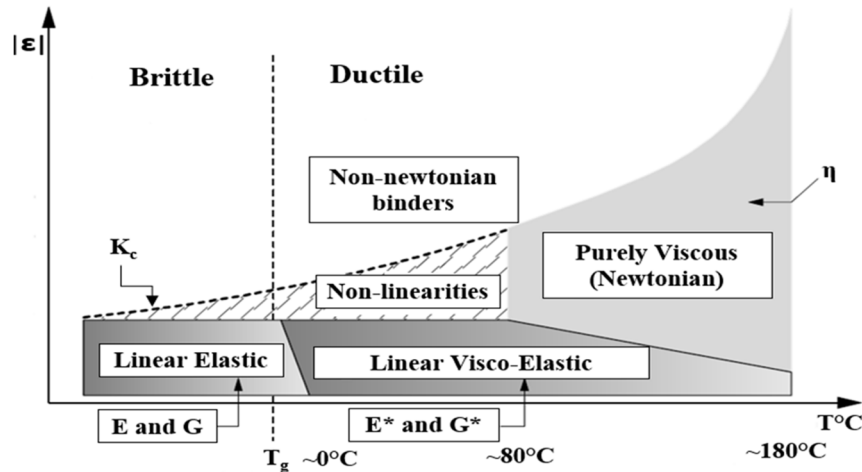
30 For economic and environmental reasons, the use of Reclaimed Asphalt Pavement (RAP) in the
31 production of new bituminous mixtures HMA (hot-mix asphalt) [1], [2], [3], [4], [5] and WMA
32 (warm-mix asphalt) [6], [7] has become a common strategy for the construction and maintenance of
33 roads.

34 Due to the long-term aging process, the physical and rheological properties as well as the
35 chemical structure of the RAP-bitumen suffer irreversible changes [8], [9]. For these reasons, in
36 order to achieve an adequate workability and good mechanical performance of a new bituminous
37 mixture containing RAP material, a softer bitumen [10], [11] or some rejuvenators [12], [13], [14],
38 [15], [16], [17] could be used.

39 Many studies showed the efficiency of using vegetal oils by evaluating the conventional
40 properties (such as penetration, ductility, Fraass temperature, ring and ball temperature), fatigue or
41 complex modulus of final blends produced with these products, different RAP binders and different
42 base fresh binders [1], [18], [19], [20], [21], [22].

43 The binder has a very complex thermomechanical behaviour that is influenced by the
 44 temperature, the speed and the of the load level. In a width range of loading the behaviour can be
 45 considered as linear viscoelastic [23]. The linear viscoelastic response of a binder is commonly
 46 analysed in terms of complex shear modulus.

47 Di Benedetto and Corté (2005) indicated different behaviors of bituminous materials based on
 48 the temperature (T) and the amplitude of the deformation ($|\epsilon|$). As it can be observed in Figure 1, the
 49 following behaviors of binders can be distinguished: the brittle and the ductile domains, the linear
 50 elastic behavior (characterized by E and G), the linear viscoelastic (LVE) domain (characterized by
 51 E^* and G^*), the purely viscous Newtonian behavior (characterized by the viscosity η), the fragile
 52 rupture (characterized by the toughness K_c) and the non-linear domain.



53

54 Figure 1. Binder behaviors as a function of T and $|\epsilon|$ [23].

55 The relation between temperature and viscosity is very important in the context of determining
 56 and evaluating some characteristics such as adhesion, rheology, durability, etc. of binders.

57 Therefore, the characterization and the understanding of the viscoelastic behaviour of binders it
 58 can be considered essential in the design process of a bituminous mixture due to the fact that the
 59 binder has an important influence on the mechanical response of the bituminous mixture [7].

60 Complex shear modulus (G^*) together with the steady and complex shear viscosities are the most
 61 important rheological properties, used to characterize the linear viscoelastic behaviour of binders.
 62 Viscosity is a fundamental characteristic property of binders and rejuvenators and it can be
 63 determined by several methods [24], [25], [26].

64 The complex viscosity (η^*) determined by oscillatory test is defined as the ratio between the
 65 complex shear modulus G^* and the angular frequency ω , multiplied by i ($i^2 = -1$).

66 Steady shear viscosity (η_0) at a given temperature corresponds to the limit of the norm of the
 67 complex viscosity $|\eta^*|$ when angular frequency ω tends towards zero.

68 The objective of this paper is to study the properties of several binder blends between one type
 69 of fresh binder, a RAP binder with/without a rejuvenator of vegetal origin by evaluating the steady
 70 shear viscosity at different temperatures ($\eta_0(T)$). The experimental plan includes seventeen
 71 binders. The materials used are specific for Romania.

72 In addition, steady shear viscosity values of all binder blends were estimated with two different
 73 approaches from values of $\eta_0(T)$ of the base constituents. Correlation plots between the
 74 experimental and estimated results (with both approaches) were analysed in order to verify if these
 75 two estimation approaches are valid for these tested binders. Similar estimation methods were used
 76 in order to estimate the conventional properties of the same binder blends in [27].

77

78 **2. Materials**

79 Three base materials were used: one type of fresh binder (a 50/70 pen. grade binder), a RAP binder
 80 (extracted and recovered from a RAP material) and one type of rejuvenator (a mixture of vegetal
 81 oils).

82 The RAP material was classified and described by performing the tests required by EN 13108-8
 83 [28]. Its measured binder content is 4.0%.

84 The rejuvenator (Rej) was used in four dosages from 0% to 15% by mass of RAP binder (with a
 85 5% increment) corresponding to 0.0%, 0.2%, 0.4% and 0.6% by mass of the RAP material.

86 The experimental campaign considers 17 binders: 15 blends (12 blends of the three base
 87 materials and 3 blends between the base RAP binder and the rejuvenator) and the two base binders
 88 (Table 1). It must be mentioned that different properties of the same binder blends were analysed in
 89 Forton et. al [27, 29].

90 Proportions of these three base components (RAP binder, fresh binder and rejuvenator) were
 91 calculated in order to reproduce real ratios within corresponding bituminous mixtures (having a
 92 total binder content 5.6%) containing 25%, 50%, 75% and 100% RAP material and different
 93 dosages of Rej. A summary table regarding the proportions for all binders is reported in Table 1.

94 To simplify, binder blends were named according to the penetration grade of the fresh bitumen
 95 (50/70), the dosage of RAP material used for the production of bituminous mixture (25%, 50%,
 96 75%) and the dosage of the rejuvenator by the mass of RAP bitumen (5%, 10%, 15%).

97 Table 1. Weight proportion of the three base materials (fresh and RAP binders and the rejuvenator)
 98 in tested binders [24]

Bitumens	weight proportion in percent (%)		
	50/70	RAP	Rej
50/70	100.0	-	-
RAP	-	100.0	-
RAP + 5% Rej	-	95.2	4.8
RAP + 10% Rej	-	90.9	9.1
RAP + 15% Rej	-	87.0	13.0
50/70 + 25% RAP	82.1	17.9	-
50/70 + 50% RAP	64.3	35.7	-
50/70 + 75% RAP	46.4	53.6	-
50/70 + 25% RAP + 5% Rej	81.4	17.7	0.9
50/70 + 50% RAP + 5% Rej	63.1	35.1	1.8
50/70 + 75% RAP + 5% Rej	45.22	52.17	2.61
50/70 + 25% RAP + 10% Rej	80.7	17.5	1.8
50/70 + 50% RAP + 10% Rej	62.1	34.5	3.4
50/70 + 75% RAP + 10% Rej	44.1	50.8	5.1
50/70 + 25% RAP + 15% Rej	80.0	17.4	2.6
50/70 + 50% RAP + 15% Rej	61.0	33.9	5.1
50/70 + 75% RAP + 15% Rej	43.0	49.6	7.4

99 The procedures used to produce the studied binder blends were chosen in order to reproduce in
 100 laboratory the actual production process of bituminous mixtures containing RAP material and
 101 rejuvenator.

102 Therefore, the fresh and RAP binders were heated at 160°C in a thermostatic oven. The
 103 rejuvenator was not heated before blending. All binder blends were produced in two steps. First, the
 104 rejuvenator (at ambient temperature) was added to fresh binder (which was heated for 30 min) and
 105 this preliminary blend was manually mixed for 5 minutes. This blend was than heated for 20 min at

106 160°C. Secondly, the RAP binder was added, and this final blend was manually mixed for 5
107 minutes in order to produce a homogenous blend. The 160°C temperature was chosen with respect
108 to the Romanian technical specifications for the production of bituminous mixtures.

109 3. Experimental campaign

110 3.1 Complex shear modulus test

111 A DSR apparatus with a 25 mm diameter plate-plate configuration with a 1 mm gap was used at
112 temperatures ranging from 25°C to 85°C and at frequencies ranging from 0.1 Hz to 10 Hz.

113 As all the tests, for all considered binder blends, were performed at intermediate and high
114 temperatures, a 5% shear strain amplitude, which is the Linear Visco-Elastic domain according to
115 Airey, Rahimzadeh & Collop (2003) [30], was imposed.

116 Tests were performed at 5% targeted shear strain amplitude (γ), by imposing a sinusoidal shear
117 strain signal and measuring the corresponding shear stress. However, the torque limit of the
118 instrument was reached for strain amplitudes lower than the 5% targeted value during some tests at
119 the lowest temperatures and highest frequencies [29]. Therefore, these tests were performed at
120 strain amplitudes lower than 5%.

121 In order to highlight the influence of RAP binder and Rej content on the behaviour of the final
122 blends, master curves of norm of complex shear modulus $|G^*|$ were built for all blends at a
123 reference temperature of $T_{ref} = 85^\circ\text{C}$. The Time–Temperature Superposition Principle (TTSP) was
124 applied and verified for all binders, temperature shift factors (a_T) were obtained and the master
125 curves were plotted for all binders according to equation 1 [9], [27], [31], [32], [33].

$$|G^*(T, f)| = |G^*(T_{ref}, a_T \cdot f)| \quad (1)$$

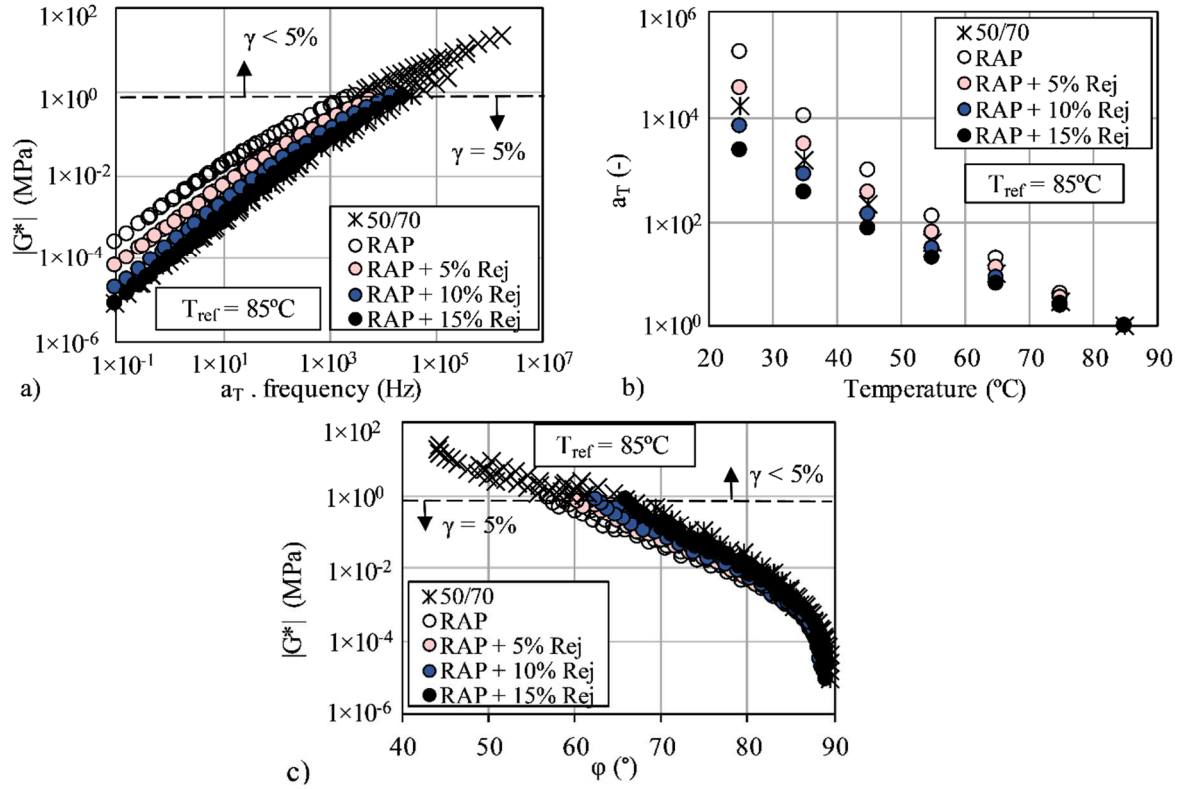
126 where T is the test temperature, T_{ref} is the reference temperature and f is the frequency.

127 Master curves of $|G^*|$ and shift factors a_T at a reference temperature of 85°C for the two base
128 binders and RAP + Rej blends are shown in Figure 2 a and b, as an example. Data obtained at low
129 temperature/high frequency during cycles performed at variable strain amplitude γ (lower than the
130 targeted 5% value) are plotted with crossed (\times).

131 The data presented in Black diagram (Figure 2 c) are located on a unique curve for each of the
132 considered blends. It means that the time temperature superposition principle (TTSP) is valid for all
133 tested binders. Then they are thermorheologically simple even when containing the rejuvenator.

134 It is observed that with increasing Rej content in the blends, the master curves of RAP + Rej
135 blends progressively approach the one of the pure bitumen. The same tendency was observed for
136 the a_T shift factors, with blends RAP + 10% Rej and RAP + 15% Rej having even lower a_T values
137 than fresh 50/70 binder. Shift factor values a_T at a reference temperature of 85°C for all binders are
138 reported in Table A.1 (Appendix). Similar tendencies were observed in Forton et. al [27, 29] for the
139 blends produced with fresh binder, 50% RAP and different amounts of rejuvenator at a reference
140 temperature of 25°C.

141



142

143 Figure 2. DSR complex modulus test results for 50/70 binder and RAP + Rej blends: (a) master
 144 curves of $|G^*|$ at 85°C ; (b) temperature shift factors at 85°C ; (c) Black diagram.

145 3.2 Determination of steady shear viscosity at 85°C from DSR test results

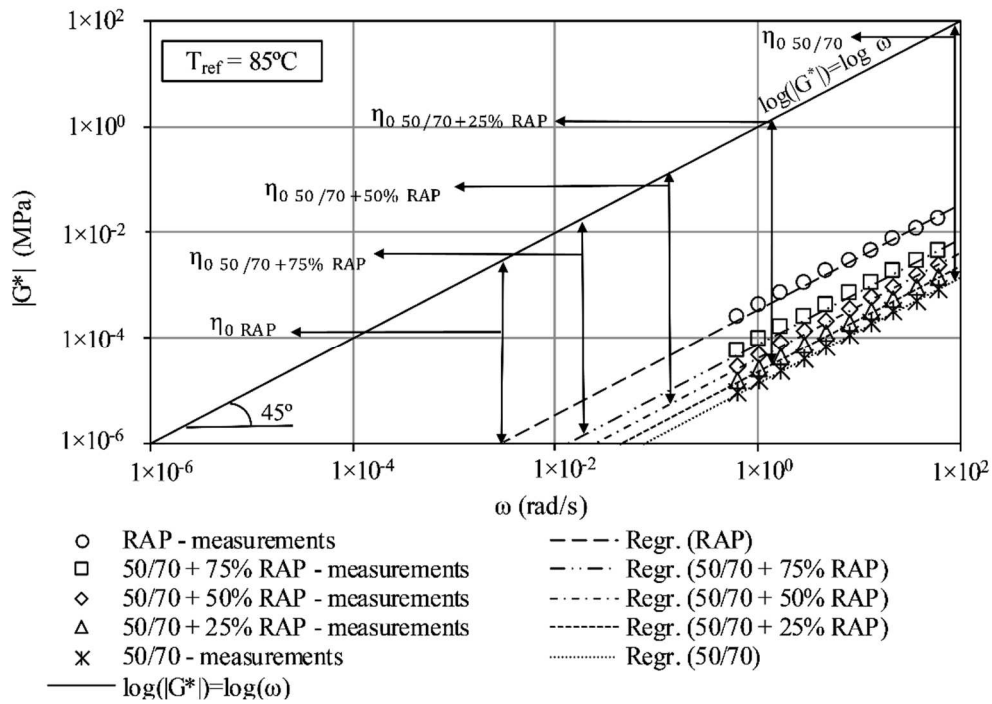
146 Steady shear viscosity (η_0) at a given temperature (85°C) corresponds to the limit of the norm of
 147 the complex viscosity $|\eta^*|$ when the angular frequency ω tends towards zero (equation 2) [27].

$$\eta_0 = |\eta^*| = \frac{|G^*|}{\omega}, \omega \rightarrow 0 \quad (2)$$

$$\log|G^*| = \log \omega + \log|\eta^*| - \text{logarithmic form of equation (2)} \quad (3)$$

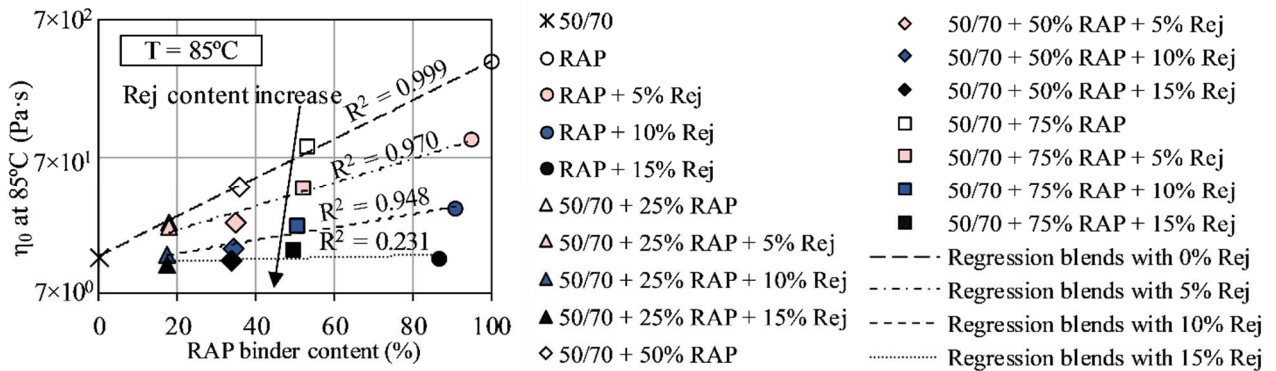
148 As an example, Figure 3 ($|G^*|$ vs. ω , in a log-log scale) shows how η_0 values were obtained, by
 149 highlighting the Newtonian behaviour by analysing the high temperature/low frequency part of the
 150 curves [27], for fresh binder, RAP binder and their blends. The obtained η_0 values for all binders
 151 are shown in Table A.1 (Appendix).

152 As it can be observed in Figure 4, η_0 values at 85°C increase with the increase of RAP binder
 153 content in the blends. Linear regressions (in logarithmic scale) could be performed on the obtained
 154 η_0 values at different temperatures with good approximation. Moreover, η_0 values decrease with the
 155 increase of rejuvenator content in the blends. These results were expected.



156

157 Figure 3. Steady shear viscosity (η_0) at 85°C of 50/70 fresh and RAP binders and their blends.



158

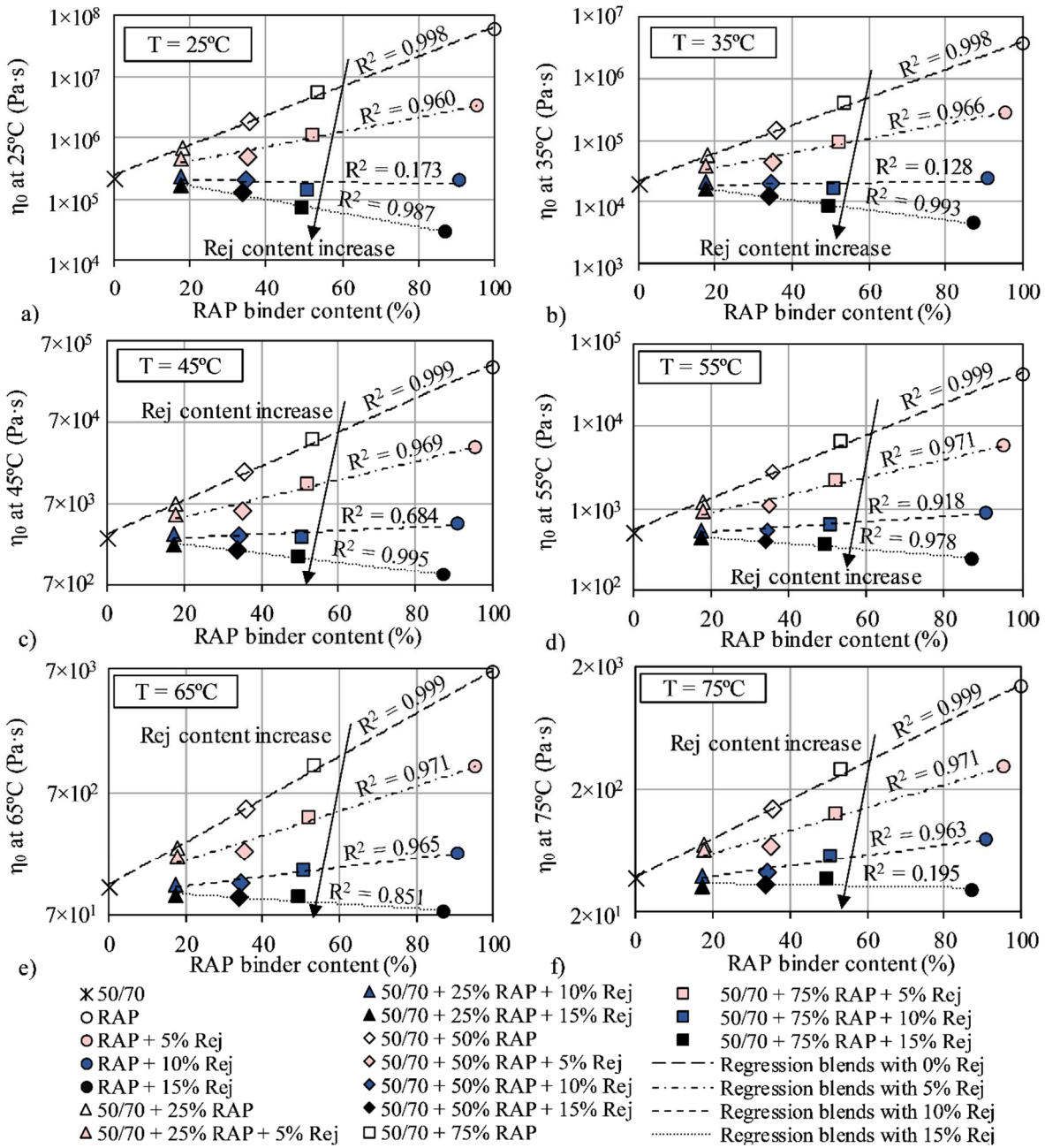
159 Figure 4. Steady shear viscosity at 85°C for all binders.

160 *3.3 Determination of steady shear viscosity at different temperatures*

161 In order to calculate η_0 values for all binders at different temperatures equation (4) was used. In this
 162 equation, the value of the steady shear viscosity at a temperature T , ($\eta_0(T)$) is calculated from the
 163 values of the steady shear viscosity at the reference temperature of 85°C, $\eta_0(T_{ref} = 85^\circ\text{C})$,
 164 multiplied by the temperature shift factor at temperature T , a_T . The same shift factors used to build
 165 $|G^*|$ master curves are used.

$$\eta_0(T) = a_T \cdot \eta_0(T_{ref}) \tag{4}$$

166 The steady shear viscosity was calculated with equation (4) for all binders at temperatures from
 167 25°C to 75°C. Results are reported in Table A.1 (Appendix) and in Figure 5.



168

169 Figure 5. Results of steady shear viscosity at different temperatures for all binders: (a) T = 25°C;
 170 (b) T = 35°C; (c) T = 45°C; (d) T = 55°C; (e) T = 65°C; (f) T = 75°C.

171 As expected, values of $\eta_0(T)$ decrease with the increase of temperature. Also, $\eta_0(T)$ increase with
 172 increasing RAP binder content in the blends and decrease with the increase of Rej content within
 173 blends. Linear regressions in logarithmic scale as a function of RAP binder content were performed
 174 with rather good approximation for all binders, at all considered temperatures. As it can be observed
 175 in Figure 5 a and b and Table A.1 (Appendix), the values of $\eta_0(T)$ at low temperatures (25°C and
 176 35°C) of the blends containing 10% Rej (independently of the RAP binder content) are close to the
 177 results obtained for the base fresh binder. This observation is not valid at higher temperatures
 178 (where $\eta_0(T)$ increases with the increasing RAP bitumen content).

179

180

181

182 4. Estimation of steady shear viscosity

183 Two approaches were proposed in order to determine the estimated values of $\eta_0(T)$ at different
184 temperatures (from 25°C to 85°C) of all produced binder blends. The obtained results were then
185 compared with the experimental values determined in Section 3.3. Similar estimation approaches
186 were used in the case of the conventional properties of same binder blends and both approaches
187 were considered valid (good correspondences were found between estimated and experimental
188 values of the European conventional parameters) [27].

189 4.1 1st approach: two-way blending rule

190 The 1st approach considers the classical blending rule expressed in equation (5), which supposes
191 that $\eta_0(T)$ values for fresh binder, RAP binder and blends of RAP + Rej (at the three different
192 dosages used in the study) are used as input values. For this approach, $\eta_0(T)$ values for RAP + Rej
193 blends must be known from experimental tests, which is a drawback as these blends should be
194 tested for each of the three considered Rej contents (5%, 10% and 15%).

195 In the equation (5), known as log-log rule, [34], the estimated value of η_0 of any of the 12 blends
196 at a given temperature ($\eta_{blend\ est.\ 1}(T)$) is determined from the experimental results of fresh binder
197 $\eta_0(T)_{(50/70)}$, and RAP + Rej blends, $\eta_0(T)_{(RAP+Rej)}$, as a function of the relative mass
198 concentration a of fresh binder in the blend.

$$\log \eta_{blend\ est.\ 1}(T) = a \cdot \log \eta_0(T)_{(50/70)} + (1 - a) \cdot \log \eta_0(T)_{(RAP+Rej)} \quad (5)$$

199 4.2 2nd approach: three-way blending rule

200 The 2nd approach consists in the three-way blending rule expressed in equation (6), which requires
201 as input data only the values of $\eta_0(T)$ for the three base materials used in this study.

202 The estimated values of steady shear viscosity at a given temperature for any of the 15 blends
203 ($\eta_{blend\ est.\ 2}(T)$) were calculated from the experimental results of fresh binder ($\eta_0(T)_{(50/70)}$), RAP
204 binder ($\eta_0(T)_{(RAP)}$) and from equivalent values of the rejuvenator ($\eta_0(T)_{(Rej)}$).

$$\log \eta_{blend\ est.\ 2}(T) = a \cdot \log \eta_0(T)_{(50/70)} + b \cdot \log \eta_0(T)_{(RAP)} + c \cdot \log \eta_0(T)_{(Rej)} \quad (6)$$

205 where a , b and c are the relative mass concentrations of the three base materials, respectively ($a +$
206 $b + c = 1$).

207 Equation (6) could be rewritten as equation (7), considering that a and c could be calculated as
208 functions of b and of the percentage of Rej by the mass of RAP binder, r ($c = r \cdot b$).

$$\log \eta_{blend\ est.\ 2}(T) = [1 - b \cdot (1 + r)] \cdot \log \eta_0(T)_{(50/70)} + b \cdot \log \eta_0(T)_{(RAP)} + b \cdot r \cdot \log \eta_0(T)_{(Rej)} \quad (7)$$

209 In order to obtain the equivalent values for the rejuvenator of ($\eta_0(T)_{(Rej)}$) at a given
210 temperature, it was necessary to optimize the correlation between experimental results and
211 estimated values of blends ($\eta_{blend\ est.\ 2}(T)$). The least square method was used by maximizing the
212 R^2 value of the estimated vs. experimental correlation in order to obtain $\eta_0(T)_{(Rej)}$. It should be
213 mentioned that these equivalent $\eta_0(T)_{(Rej)}$ values were used only for this second estimation
214 approach, which is valid only for rather small Rej content (up to 15%). This equivalent viscosity is
215 not equal to the viscosity of the rejuvenator used for this study.

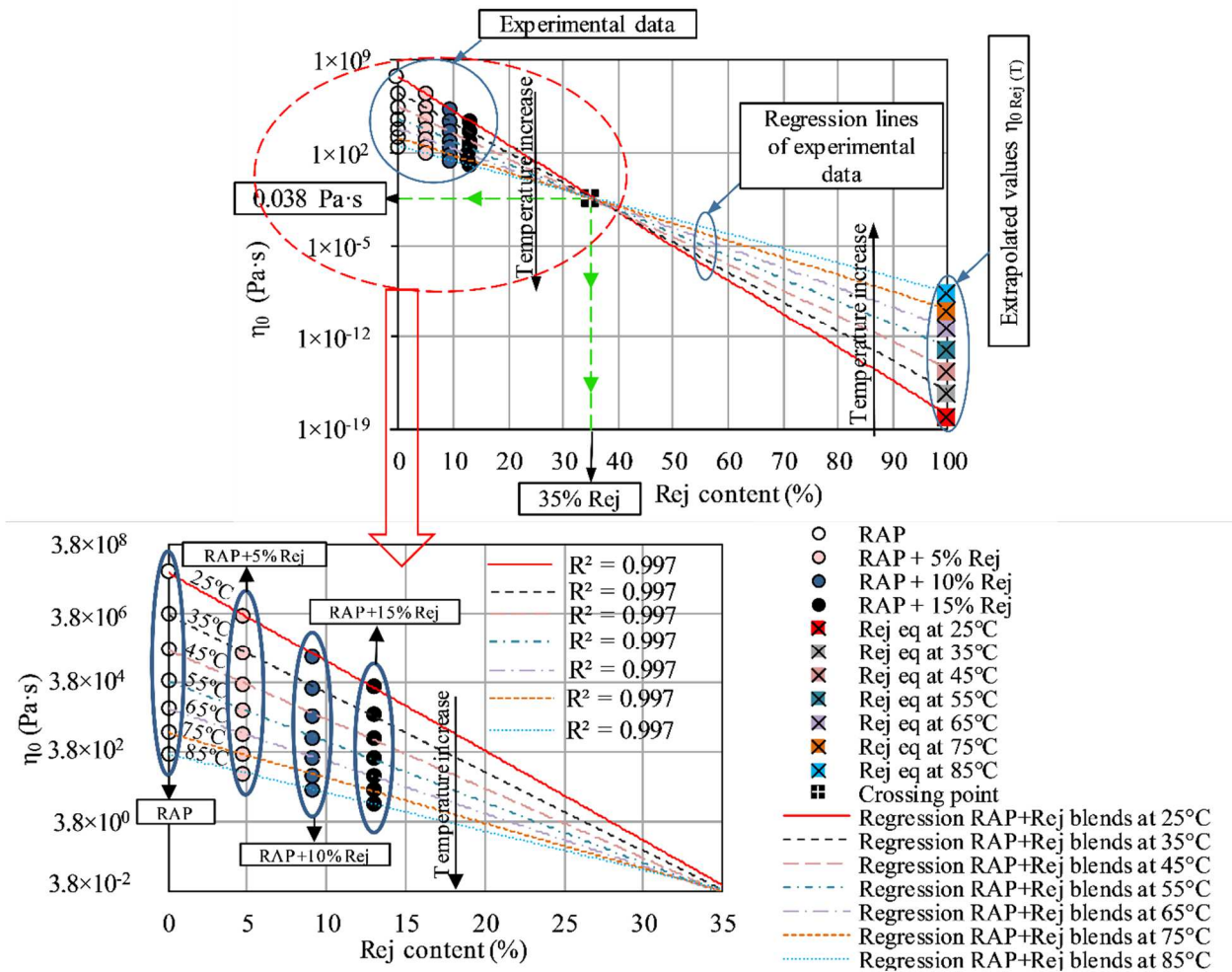
216 In Figure 6, the experimental results of η_0 at different temperatures for RAP + Rej blends are
217 plotted as a function of the rejuvenator content, together with the equivalent values of $\eta_0(T)_{(Rej)}$
218 determined for the rejuvenator. Linear regressions could be performed with excellent approximation
219 at all considered temperatures. It was observed that all the regression lines can be obtained with the
220 same R^2 (influence only on the 4th decimal) when considering that all lines intersect a unique point:
221 35% Rej content and 0.038 Pa·s. Figure 6 gives an overview of these results.

222 These results led to the idea of a “temperature-independent constant content-viscosity couple”
 223 for the rejuvenator which is expressed in Equations (8) and (9), where viscosity is expressed in Pa.s.
 224 Equation (8) is in fact equation (6) in which the amount of the fresh binder is equal to zero and
 225 $\eta_{blend\ est.\ 2}(T) = \eta_{RAP+35\% Rej} = 0.038\ Pa \cdot s$. Equation (7) can then be rewritten as in equation (10),
 226 consisting in the final form of the 2nd approach when viscosity is expressed in Pa.s.

$$\log 0.038 = 0.65 \log \eta_0(T)_{(RAP)} + 0.35 \log \eta_0(T)_{(Rej)} \quad (8)$$

$$\log \eta_0(T)_{(Rej)} = \frac{\log 0.038}{0.35} - \frac{0.65}{0.35} \log \eta_0(T)_{(RAP)} \quad (9)$$

$$\log \eta_{blend\ est.\ 2}(T) = [1 - b(1 + r)] \log \eta_0(T)_{(50/70)} + b \left(1 - \frac{0.65}{0.35} r\right) \log \eta_0(T)_{(RAP)} + \frac{b \cdot r}{0.35} \log 0.038 \quad (10)$$



227
 228 Figure 6. Experimental results of $\eta_0(T)$ for RAP + Rej blends, equivalent values for rejuvenator
 229 $\eta_0(T)_{(Rej)}$, plotted as a function of Rej content in the blends, at all considered temperatures.

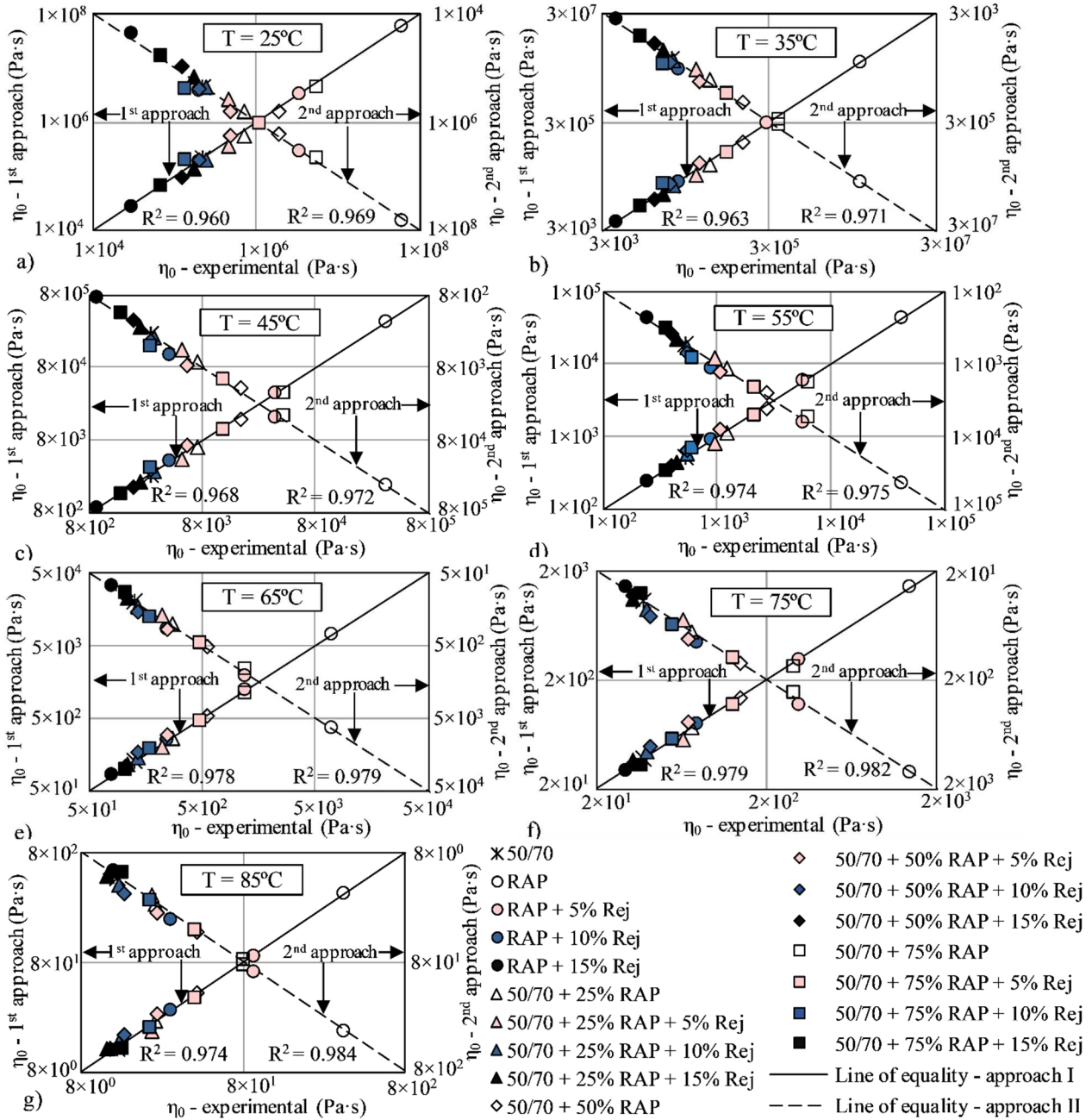
230 **4.3 Analysis of results**

231 Plots of the estimated results obtained from the 1st approach and the 2nd approach versus the
 232 experimental results are and shown in Figure 7. Estimated results of $\eta_0(T)$ of all blends are reported
 233 in Table A.2 and Table A.3 (Appendix).

234 The coefficient of determination (R^2) was calculated for each plot with respect to the equality
 235 line.

236
237
238
239
240
241

In order to calculate R^2 for the 1st approach, steady shear viscosity values of the base constituents (fresh 50/70 binder, RAP binder and the three RAP + Rej blends, for a total of five binders) were not taken into account. Regarding the 2nd approach, R^2 was calculated without considering the steady shear viscosity values of the base constituents: fresh 50/70 binder, RAP binder and the ‘temperature-independent constant content-viscosity couple’ for the rejuvenator. These values are not considered because they correspond to input data, which are perfectly estimated.



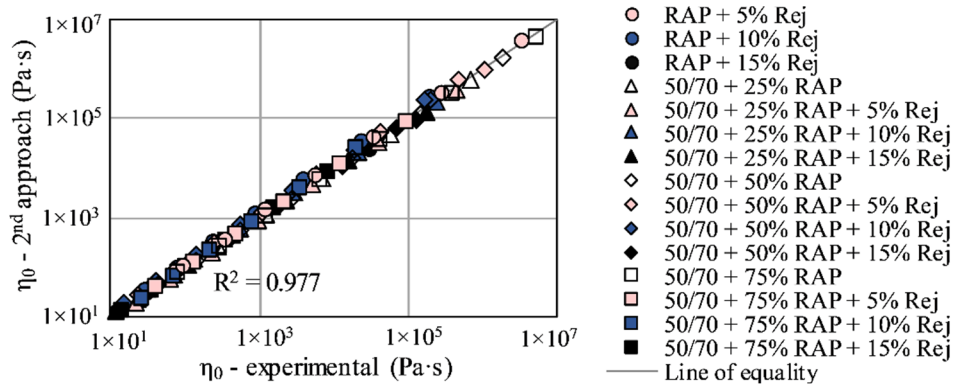
242

243 Figure 7. Plots of estimated vs. experimental results of steady shear viscosity for all binder blends:
 244 (a) $T = 25^\circ\text{C}$; (b) $T = 35^\circ\text{C}$; (c) $T = 45^\circ\text{C}$; (d) $T = 55^\circ\text{C}$; (e) $T = 65^\circ\text{C}$; (f) $T = 75^\circ\text{C}$; (g) $T = 85^\circ\text{C}$.

245 As it can be observed in Figure 7, the estimated results ($\eta_{blend\ est.\ 1}(T)$, $\eta_{blend\ est.\ 2}(T)$) of all
 246 binder blends are close to the corresponding experimental results. It can be noticed that with the
 247 decrease of temperature (from 85°C to 25°C) R^2 values decrease but they are still satisfactory
 248 (always higher than 0.960).

249 R^2 values obtained in the case of the 2nd approach are always higher than 0.969 and greater than
 250 the values obtained with the 1st approach. Considering the goodness of the correlation with
 251 experimental points and the reduced number of input data necessary, the 2nd approach can be
 252 considered more advantageous than the 1st approach.

253 As a general comment, with the 2nd approach a total of 105 η_0 values were estimated, at seven
 254 different temperatures for 15 blends, using as input data the experimental results of η_0 obtained at a
 255 reference temperature of 85°C, $\eta_0(T_{ref} = 85^\circ\text{C})$, for fresh and RAP binders and the ‘temperature-
 256 independent constant couple’ for the rejuvenator. A global correlation plot between all these
 257 estimated values obtained by applying the 2nd approach and the experimental values of the 15
 258 blends is shown in Figure 8. A satisfactory global R^2 was found (0.977).



259
 260 Figure 8. Global correlation plot of estimated (2nd approach) vs. experimental results of $\eta_0(T)$ at
 261 temperatures from 85°C to 25°C for the 15 blends of fresh 50/70, RAP binders and rejuvenator
 262 (Rej).

263 5. Conclusions

264 The objectives of the presented work were to study the influence of the addition of a rejuvenator of
 265 vegetal origin on the steady shear viscosity of binder blends of fresh and RAP binders and to
 266 propose two approaches in order to estimate η_0 of all blends from experimental results obtained for
 267 the base constituents.

268 Three base materials were used in this study: one type of pure bitumen (50/70), a RAP bitumen
 269 and a rejuvenator, which were blended in different proportions, producing 17 binders (including the
 270 two base bitumens).

271 Complex shear modulus tests were performed on all binders at temperatures from 25°C to 85°C
 272 and at frequencies from 0.1 Hz to 10 Hz. The Time-Temperature Superposition Principle was
 273 validated for all tested binders. Steady shear viscosity (η_0) at 85°C was obtained as the norm of
 274 complex viscosity at high temperature/low frequency in the domain of Newtonian behaviour of
 275 binders. η_0 values at temperatures from 75°C to 25°C were calculated from the experimental values
 276 of η_0 at the reference temperature of 85°C, ($\eta_0(T_{ref} = 85^\circ\text{C})$), multiplied by the shift factors. Two
 277 different estimation approaches were proposed and η_0 values were estimated for all produced
 278 binder blends at all temperatures from 25°C to 85°C, from η_0 values of base constituents.

279 From the obtained results it can be concluded that, for all temperatures, η_0 values are increasing
 280 with the increase of RAP binder content and with the decrease of Rej content in the blends. The
 281 addition of the rejuvenator was observed to counterbalance the stiffening effect of the RAP binder
 282 in the blends. These effects that were expected are clearly quantified and well estimated by the two
 283 proposed approaches.

284 Slightly better correspondence was found between estimated η_0 values obtained with the 2nd
 285 approach, which is an original input of this work, and experimental values (R^2 values always higher
 286 than those found with the 1st approach, which is based on the classical log-log rule). Moreover, the

287 2nd approach has also the great advantage to need only one data for each of the three base
288 constituents when the dosage is fixed.
289
290

291 6. References

- 292 [1] Mazzoni, G., Bocci, E., Canestrari, F., 2018. Influence of rejuvenators on bitumen ageing in
293 hot recycled asphalt mixtures. *Journal of Traffic and Transportation Engineering (English*
294 *Edition)*, VI. 5, Issue 3, 157-168. <https://doi.org/10.1016/j.jtte.2018.01.001>.
- 295 [2] Yin, F., Kaseer, F., Arambula-Mercado, E., Epps Martin, A., 2017. Characterising the long-
296 term rejuvenating effectiveness of recycling agents on asphalt blends and mixtures with high
297 RAP and RAS contents. *Road Materials and Pavement Design*, 18:4, 273-
298 292. <https://doi.org/10.1080/14680629.2017.1389074>.
- 299 [3] Tapsoba, N., Sauzéat, C., Di Benedetto, H., Baaj, H., Ech, M., 2014. Behaviour of asphalt
300 mixtures containing reclaimed asphalt pavement and asphalt shingle. *Road Materials and*
301 *Pavement Design*, 15:2, 330-347. <https://doi.org/10.1080/14680629.2013.871091>.
- 302 [4] Hong, F., Prozzi, J.A., 2018. Evaluation of recycled asphalt pavement using economic,
303 environmental, and energy metrics based on long-term pavement performance sections. *Road*
304 *Materials and Pavement Design*, 19:8, 1816-1831.
305 <https://doi.org/10.1080/14680629.2017.1348306>.
- 306 [5] Moon, K.H., Falchetto, A.C., Marasteanu, M., Turos, M., 2014. Using recycled asphalt
307 materials as an alternative material source in asphalt pavements. *KSCCE Journal of Civil*
308 *Engineering*, 18:149. <https://doi.org/10.1007/s12205-014-0211-1>.
- 309 [6] Song, W., Huang, B., Shu, X., 2018. Influence of warm-mix asphalt technology and
310 rejuvenator on performance of asphalt mixtures containing 50% reclaimed asphalt pavement.
311 *Journal of Cleaner Production*, vol. 192, 191-198, ISSN 0959-6526.
312 <https://doi.org/10.1016/j.jclepro.2018.04.269>.
- 313 [7] Sun, Y., Wang, W., Chen, J., 2019. Investigating impacts of warm-mix asphalt technologies
314 and high reclaimed asphalt pavement binder content on rutting and fatigue performance of
315 asphalt binder through MSCR and LAS tests. *Journal of Cleaner Production*, vol. 219, 879-
316 893, ISSN 0959-6526. <https://doi.org/10.1016/j.jclepro.2019.02.131>.
- 317 [8] Grilli, A., Gnisci, M.I., Bocci, M., 2017. Effect of ageing process on bitumen and rejuvenated
318 bitumen. *Construction and Building Materials*, Vol: 136, pp: 474-481.
319 <https://doi.org/10.1016/j.conbuildmat.2017.01.027>
- 320 [9] Saboo, N., Kumar, P., 2016. Use of flow properties for rheological modeling of bitumen.
321 *International Journal of Pavement Research and Technology*, 9(1), 63–72.
322 <https://doi.org/10.1016/J.IJPRT.2016.01.005>
- 323 [10] Mogawer, W.S., Fini, E.H., Austerman, A.J., Booshehrian, A., Zada, B., 2016. Performance
324 characteristics of high reclaimed asphalt pavement containing bio-modifier. *Road Materials*
325 *and Pavement Design*, 17:3, 753-767. <https://doi.org/10.1080/14680629.2015.1096820>.
- 326 [11] Liu, G., Nielsen, E., Komacka, J., Leegwater, G., Van de Ven, M., 2015. Influence of soft
327 bitumens on the chemical and rheological properties of reclaimed polymer-modified binders
328 from the old surface-layer asphalt. *Construction and Building Materials*, vol: 79, pp: 129–135.
329 <https://doi.org/10.1016/j.conbuildmat.2015.01.002>.
- 330 [12] Zaumanis, M., Mallick, R.B., Frank, R., 2014. Determining optimum rejuvenator dose for
331 asphalt recycling based on Superpave performance grade specifications. *Construction and*
332 *Building Materials*, 69, 155e166. <https://doi.org/10.1016/j.conbuildmat.2014.07.035>.
- 333 [13] Yu, X., Zaumanis, M., Dos Santos, S., Poulidakos, L., 2014. Rheological, microscopic, and
334 chemical characterization of the rejuvenating effect on asphalt binders. *Fuel*, vol: 135, pp:
335 162–171, <https://doi.org/10.1016/j.fuel.2014.06.038>.

- 336 [14] Chen, J.S., Huang, C.C., Chu, P.Y., Lin, K.Y., 2007. Engineering characterization of recycled
 337 asphalt concrete and aged bitumen mixed recycling agent. *Journal of Materials Science*,
 338 Volume 42, Number 23, Page 9867. <https://doi.org/10.1007/s10853-007-1713-8>.
- 339 [15] Hajj, E., Souliman, M., Alavi, M., Salazar, L.G.L., 2013. Influence of hydrogreen bioasphalt
 340 on viscoelastic properties of reclaimed asphalt mixtures. *Transportation Research*
 341 *Record*, 2371, 13-22. <https://doi.org/10.3141/2371-02>.
- 342 [16] Shen, J., Amirkhanian, S., Miller, J.A., 2007. Effects of Rejuvenating Agents on Superpave
 343 Mixtures Containing Reclaimed Asphalt Pavement. *Journal of Materials in Civil*
 344 *Engineering*, 19:5. [https://doi.org/10.1061/\(ASCE\)0899-1561\(2007\)19:5\(376\)](https://doi.org/10.1061/(ASCE)0899-1561(2007)19:5(376)).
- 345 [17] Behnood, A., 2019. Application of rejuvenators to improve the rheological and mechanical
 346 properties of asphalt binders and mixtures: A review. *Journal of Cleaner Production*, vol.
 347 231, 171-182, ISSN 0959-6526. <https://doi.org/10.1016/j.jclepro.2019.05.209>.
- 348 [18] Bailey, H.K., Zoorobo, S.E., 2012. The use of vegetable oil in asphalt mixtures, in laboratory
 349 and field. *5th Eurobitume- Euroasphalt Congress*. Istanbul.
- 350 [19] Mangiafico, S., Sauzéat, C., Di Benedetto, H., Pouget, S., Olard, F., Planque, L., 2017.
 351 Complex modulus and fatigue performances of bituminous mixtures with reclaimed asphalt
 352 pavement and a recycling agent of vegetable origin. *Road Materials and Pavement Design*,
 353 18:2, 315-330. <https://doi.org/10.1080/14680629.2016.1213509>.
- 354 [20] Mogawer, W.S., Booshehrian, A., Vahidi, S., Austerman, A.J., 2013. Evaluating the effect of
 355 rejuvenators on the degree of blending and performance of high RAP, RAS, and RAP/RAS
 356 mixtures. *Road Materials and Pavement Design*, 14:2, 193-213.
 357 <https://doi.org/10.1080/14680629.2013.812836>.
- 358 [21] Noferini, L., Simone, A., Sangiorgi, C., Mazzotta, F., 2017. Investigation on performances of
 359 asphalt mixtures made with Reclaimed Asphalt Pavement: Effects of interaction between
 360 virgin and RAP bitumen. *International Journal of Pavement Research and Technology*, 10:4,
 361 322-332. <https://doi.org/10.1016/j.ijprt.2017.03.011>.
- 362 [22] Oldham, D., Hung, A., Parast, M., Fini, E., 2018. Investigating bitumen rejuvenation
 363 mechanisms using a coupled rheometry-morphology characterization approach. *Construction*
 364 *and Building Materials*, 159, 37-45. <https://doi.org/10.1016/j.conbuildmat.2017.10.113>.
- 365 [23] Corté, J.F., & Di Benedetto H., 2005. *Matériaux routiers bitumineux 1: Description et*
 366 *propriétés des constituants* [Bituminous paving materials 1: Description and constituent
 367 properties]. Paris: Hermes-Lavoisier. [in French]
- 368 [24] Sahasrabudhe, S.N., Rodriguez-Martinez, V., O'Meara, M., Farkas, B.E., 2017. Density,
 369 viscosity, and surface tension of five vegetable oils at elevated temperatures: Measurement
 370 and modelling. *International Journal of Food Properties*, 20:sup2, 1965-1981,
 371 <https://doi.org/10.1080/10942912.2017.1360905>.
- 372 [25] Nivitha, M.R., Murali Krishnan, J., 2018. Rheological characterisation of unmodified and
 373 modified bitumen in the 90–200°C temperature regime. *Road Materials and Pavement*
 374 *Design*, 1-18. <https://doi.org/10.1080/14680629.2018.1552890>.
- 375 [26] Hashim Nierat, T., Musameh, S., Ashqer, I., 2014. Temperature-dependence of olive oil
 376 viscosity. *Materials Science*, 11(7):233-238.
- 377 [27] Forton, A., Mangiafico, S., Sauzéat, C., Di Benedetto, H., Marc, P., 2020. Properties of blends
 378 of fresh and RAP binders with rejuvenator: Experimental and estimated results. *Construction*
 379 *and Building Materials*, 236:117555 (2020),
 380 <https://doi.org/10.1016/j.conbuildmat.2019.117555>.
- 381 [28] EN 13108-8:2016 Standard. 2016. *Bituminous mixtures- part 8: Reclaimed asphalt*.
- 382 [29] Forton, A., Mangiafico, S., Sauzéat, C., Di Benedetto, H., Marc, P., 2019. Rheological
 383 properties of fresh and RAP bitumen blends with or without regenerating agent. *Conference:*
 384 *7th International Conference on Bituminous Mixtures and Pavements, Thessaloniki, Greece*,
 385 DOI: 10.1201/9781351063265-2.
- 386 [30] Airey, G. D., Rahimzadeh, B., & Collop, A. C., 2003. Viscoelastic limits for bituminous

- 387 materials. *Materials and Structures*, 36, 643-647. <https://doi.org/10.1007/BF02479495>.
- 388 [31] Di Benedetto, H., Neifar, M., Sauzéat, C., Olard, F., 2007. Three-dimensional thermo-
389 viscoplastic behaviour of bituminous materials: The DBN model. *Road Materials and*
390 *Pavement Design*, 8, 285–316. <https://doi.org/10.1080/14680629.2007.9690076>.
- 391 [32] Mangiafico, S., Sauzéat, C., Di Benedetto, H., 2019. Comparison of different blending
392 combinations of virgin and RAP-extracted binder: Rheological simulations and statistical
393 analysis. *Construction and Building Materials*, VI. 197, 454-463.
394 DOI: 10.1016/j.conbuildmat.2018.11.217.
- 395 [33] Pouget, S., Sauzéat, C., Di Benedetto, H., Olard, F., 2010. From the Behavior of Constituent
396 Materials to the Calculation and Design of Orthotropic Bridge Structures. *Road Materials and*
397 *Pavement Design*, 11:1, 111-144. <https://doi.org/10.1080/14680629.2010.9690329>.
- 398 [34] Mangiafico, S., Di Benedetto, H., Sauzéat, C., Olard, F., Pouget, S., Planque, L., 2014. New
399 method to obtained viscoelastic properties of bitumen blends from pure and reclaimed asphalt
400 pavement binder constituents. *Road Materials and Pavement Design*, 15:2, 312-329.
401 <https://doi.org/10.1080/14680629.2013.870639>.
- 402

403 **Acknowledgement**

404 This research did not receive any specific grant from funding agencies in the public, commercial, or
405 not-for-profit sectors.

Appendix

Table A.1. a_T shift factors values at a reference temperature of 85°C and experimental results of steady shear viscosity, $\eta_0(T)$, at different temperatures for all tested binders.

Binders	a_T (-) at $T_{ref} = 85^\circ\text{C}$							$\eta_0(T)$, (Pa·s)						
	85°C	75°C	65°C	55°C	45°C	35°C	25°C	85°C	75°C	65°C	55°C	45°C	35°C	25°C
50/70	1	2.87×10 ⁰	9.65×10 ⁰	3.95×10 ¹	2.08×10 ²	1.51×10 ³	1.67×10 ⁴	1.32×10 ¹	3.79×10 ¹	1.27×10 ²	5.22×10 ²	2.74×10 ³	1.99×10 ⁴	2.21×10 ⁵
RAP	1	4.14×10 ⁰	2.05×10 ¹	1.26×10 ²	9.96×10 ²	1.09×10 ⁴	1.77×10 ⁵	3.39×10 ²	1.41×10 ³	6.96×10 ³	4.26×10 ⁴	3.38×10 ⁵	3.69×10 ⁶	6.01×10 ⁷
RAP + 5% Rej	1	3.33×10 ⁰	1.30×10 ¹	6.17×10 ¹	3.72×10 ²	3.02×10 ³	3.59×10 ⁴	9.36×10 ¹	3.12×10 ²	1.22×10 ³	5.78×10 ³	3.48×10 ⁴	2.83×10 ⁵	3.36×10 ⁶
RAP + 10% Rej	1	2.70×10 ⁰	8.40×10 ⁰	3.09×10 ¹	1.41×10 ²	8.33×10 ²	6.97×10 ³	2.90×10 ¹	7.84×10 ¹	2.44×10 ²	8.97×10 ²	4.08×10 ³	2.42×10 ⁴	2.02×10 ⁵
RAP + 15% Rej	1	2.35×10 ⁰	6.24×10 ⁰	1.94×10 ¹	7.30×10 ¹	3.52×10 ²	2.35×10 ³	1.27×10 ¹	2.99×10 ¹	7.96×10 ¹	2.47×10 ²	9.30×10 ²	4.49×10 ³	3.02×10 ⁴
50/70 + 25% RAP	1	3.14×10 ⁰	1.16×10 ¹	5.28×10 ¹	3.08×10 ²	2.47×10 ³	3.01×10 ⁴	2.31×10 ¹	7.27×10 ¹	2.69×10 ²	1.22×10 ³	7.11×10 ³	5.71×10 ⁴	6.95×10 ⁵
50/70 + 25% RAP + 5% Rej	1	2.96×10 ⁰	1.03×10 ¹	4.38×10 ¹	2.39×10 ²	1.81×10 ³	2.10×10 ⁴	2.16×10 ¹	6.39×10 ¹	2.22×10 ²	9.45×10 ²	5.17×10 ³	3.91×10 ⁴	4.54×10 ⁵
50/70 + 25% RAP + 10% Rej	1	2.90×10 ⁰	9.83×10 ⁰	4.07×10 ¹	2.16×10 ²	1.58×10 ³	1.76×10 ⁴	1.36×10 ¹	3.93×10 ¹	1.34×10 ²	5.52×10 ²	2.93×10 ³	2.14×10 ⁴	2.39×10 ⁵
50/70 + 25% RAP + 15% Rej	1	2.84×10 ⁰	9.45×10 ⁰	3.82×10 ¹	1.97×10 ²	1.40×10 ³	1.50×10 ⁴	1.14×10 ¹	3.24×10 ¹	1.08×10 ²	4.35×10 ²	2.25×10 ³	1.59×10 ⁴	1.71×10 ⁵
50/70 + 50% RAP	1	3.37×10 ⁰	1.34×10 ¹	6.54×10 ¹	4.09×10 ²	3.51×10 ³	4.51×10 ⁴	4.17×10 ¹	1.40×10 ²	5.59×10 ²	2.72×10 ³	1.71×10 ⁴	1.46×10 ⁵	1.88×10 ⁶
50/70 + 50% RAP + 5% Rej	1	3.01×10 ⁰	1.06×10 ¹	4.55×10 ¹	2.48×10 ²	1.84×10 ³	2.04×10 ⁴	2.32×10 ¹	7.00×10 ¹	2.47×10 ²	1.06×10 ³	5.76×10 ³	4.28×10 ⁴	4.74×10 ⁵
50/70 + 50% RAP + 10% Rej	1	2.82×10 ⁰	9.28×10 ⁰	3.70×10 ¹	1.88×10 ²	1.31×10 ³	1.37×10 ⁴	1.47×10 ¹	4.15×10 ¹	1.37×10 ²	5.46×10 ²	2.77×10 ³	1.93×10 ⁴	2.03×10 ⁵
50/70 + 50% RAP + 15% Rej	1	2.72×10 ⁰	8.62×10 ⁰	3.29×10 ¹	1.59×10 ²	1.05×10 ³	1.03×10 ⁴	1.21×10 ¹	3.31×10 ¹	1.05×10 ²	4.00×10 ²	1.94×10 ³	1.27×10 ⁴	1.25×10 ⁵
50/70 + 75% RAP	1	3.57×10 ⁰	1.51×10 ¹	7.87×10 ¹	5.28×10 ²	4.86×10 ³	6.69×10 ⁴	8.05×10 ¹	2.88×10 ²	1.22×10 ³	6.34×10 ³	4.25×10 ⁴	3.91×10 ⁵	5.39×10 ⁶
50/70 + 75% RAP + 5% Rej	1	3.17×10 ⁰	1.18×10 ¹	5.32×10 ¹	3.04×10 ²	2.35×10 ³	2.66×10 ⁴	4.01×10 ¹	1.27×10 ²	4.74×10 ²	2.13×10 ³	1.22×10 ⁴	9.42×10 ⁴	1.07×10 ⁶
50/70 + 75% RAP + 10% Rej	1	2.64×10 ⁰	8.02×10 ⁰	2.88×10 ¹	1.28×10 ²	7.50×10 ²	6.22×10 ³	2.13×10 ¹	5.63×10 ¹	1.71×10 ²	6.15×10 ²	2.74×10 ³	1.60×10 ⁴	1.67×10 ⁵
50/70 + 75% RAP + 15% Rej	1	2.53×10 ⁰	7.31×10 ⁰	2.51×10 ¹	1.06×10 ²	5.93×10 ²	4.74×10 ³	1.44×10 ¹	3.64×10 ¹	1.05×10 ²	3.61×10 ²	1.53×10 ³	8.54×10 ³	6.82×10 ⁴

Table A.2. Estimated values of steady shear viscosity at different temperatures from the 1st approach for all tested binder blends.
1st approach

Blends	η_0 - Steady shear viscosity (Pa·s)						
	T = 25°C	T = 35°C	T = 45°C	T = 55°C	T = 65°C	T = 75°C	T = 85°C
50/70 + 25% RAP	6.01×10^5	5.06×10^4	6.48×10^3	1.15×10^3	2.60×10^2	7.23×10^1	2.36×10^1
50/70 + 25% RAP + 5% Rej	3.66×10^5	3.26×10^4	4.40×10^3	8.16×10^2	1.94×10^2	5.60×10^1	1.90×10^1
50/70 + 25% RAP + 10% Rej	2.17×10^5	2.07×10^4	2.96×10^3	5.79×10^2	1.44×10^2	4.36×10^1	1.54×10^1
50/70 + 25% RAP + 15% Rej	1.48×10^5	1.48×10^4	2.21×10^3	4.49×10^2	1.16×10^2	3.61×10^1	1.31×10^1
50/70 + 50% RAP	1.63×10^6	1.28×10^5	1.53×10^4	2.51×10^3	5.32×10^2	1.38×10^2	4.21×10^1
50/70 + 50% RAP + 5% Rej	6.02×10^5	5.29×10^4	6.99×10^3	1.27×10^3	2.93×10^2	8.23×10^1	2.72×10^1
50/70 + 50% RAP + 10% Rej	2.13×10^5	2.14×10^4	3.19×10^3	6.41×10^2	1.63×10^2	4.99×10^1	1.78×10^1
50/70 + 50% RAP + 15% Rej	1.01×10^5	1.11×10^4	1.80×10^3	3.90×10^2	1.06×10^2	3.46×10^1	1.30×10^1
50/70 + 75% RAP	4.45×10^6	3.27×10^5	3.62×10^4	5.52×10^3	1.09×10^3	2.63×10^2	7.52×10^1
50/70 + 75% RAP + 5% Rej	9.80×10^5	8.51×10^4	1.10×10^4	1.95×10^3	4.39×10^2	1.20×10^2	3.86×10^1
50/70 + 75% RAP + 10% Rej	2.10×10^5	2.22×10^4	3.42×10^3	7.06×10^2	1.83×10^2	5.69×10^1	2.05×10^1
50/70 + 75% RAP + 15% Rej	7.07×10^4	8.15×10^3	1.48×10^3	3.41×10^2	9.74×10^1	3.31×10^1	1.29×10^1

Table A.3. Estimated values of steady shear viscosity at different temperatures from 2nd approach for all tested binder blends.

Blends	2 nd approach						
	η_0 – Steady shear viscosity (Pa·s)						
	T = 25°C	T = 35°C	T = 45°C	T = 55°C	T = 65°C	T = 75°C	T = 85°C
RAP + 5% Rej	3.37×10 ⁶	3.03×10 ⁵	3.84×10 ⁴	6.41×10 ³	1.34×10 ³	3.36×10 ²	9.85×10 ¹
RAP + 10% Rej	2.45×10 ⁵	3.11×10 ⁴	5.30×10 ³	1.14×10 ³	2.99×10 ²	9.15×10 ¹	3.20×10 ¹
RAP + 15% Rej	2.25×10 ⁴	3.90×10 ³	8.71×10 ²	2.37×10 ²	7.62×10 ¹	2.79×10 ¹	1.14×10 ¹
50/70 + 25% RAP	6.01×10 ⁵	5.06×10 ⁴	6.48×10 ³	1.15×10 ³	2.60×10 ²	7.23×10 ¹	2.36×10 ¹
50/70 + 25% RAP + 5% Rej	3.67×10 ⁵	3.31×10 ⁴	4.49×10 ³	8.33×10 ²	1.98×10 ²	5.69×10 ¹	1.92×10 ¹
50/70 + 25% RAP + 10% Rej	2.24×10 ⁵	2.16×10 ⁴	3.11×10 ³	6.06×10 ²	1.50×10 ²	4.48×10 ¹	1.56×10 ¹
50/70 + 25% RAP + 15% Rej	1.40×10 ⁵	1.43×10 ⁴	2.18×10 ³	4.46×10 ²	1.15×10 ²	3.56×10 ¹	1.28×10 ¹
50/70 + 50% RAP	1.63×10 ⁶	1.28×10 ⁵	1.53×10 ⁴	2.51×10 ³	5.32×10 ²	1.38×10 ²	4.21×10 ¹
50/70 + 50% RAP + 5% Rej	6.04×10 ⁵	5.43×10 ⁴	7.26×10 ³	1.32×10 ³	3.03×10 ²	8.48×10 ¹	2.77×10 ¹
50/70 + 50% RAP + 10% Rej	2.29×10 ⁵	2.35×10 ⁴	3.52×10 ³	7.02×10 ²	1.76×10 ²	5.29×10 ¹	1.85×10 ¹
50/70 + 50% RAP + 15% Rej	9.07×10 ⁴	1.06×10 ⁴	1.76×10 ³	3.84×10 ²	1.04×10 ²	3.37×10 ¹	1.25×10 ¹
50/70 + 75% RAP	4.45×10 ⁶	3.27×10 ⁵	3.62×10 ⁴	5.52×10 ³	1.09×10 ³	2.63×10 ²	7.52×10 ¹
50/70 + 75% RAP + 5% Rej	9.81×10 ⁵	8.83×10 ⁴	1.16×10 ⁴	2.06×10 ³	4.62×10 ²	1.25×10 ²	3.97×10 ¹
50/70 + 75% RAP + 10% Rej	2.35×10 ⁵	2.56×10 ⁴	3.97×10 ³	8.11×10 ²	2.06×10 ²	6.21×10 ¹	2.17×10 ¹
50/70 + 75% RAP + 15% Rej	5.98×10 ⁴	7.84×10 ³	1.42×10 ³	3.33×10 ²	9.49×10 ¹	3.18×10 ¹	1.22×10 ¹